

# The free license codes as Decision Support System (DSS) for the emergency planning to simulate radioactive releases in case of accidents in the new generation energy plants

Andrea Malizia<sup>1,2</sup>, Mariachiara Carestia<sup>1,2</sup>, Claudio Cafarelli<sup>2</sup>, Laura Milanese<sup>2</sup>, Simona Pagannone<sup>2</sup>, Amedeo Pappalardo<sup>2</sup>, Massimo Pedemonte<sup>2</sup>, Gianna Latini<sup>2</sup>, Oscar Barlascini<sup>2</sup>, Eugenio Fiorini<sup>2</sup>, Paolo Maurizio Soave<sup>2</sup>, Daniele Di Giovanni<sup>1,2</sup>, Orlando Cenciarelli<sup>1,2</sup>, Luca Antonelli<sup>1,2</sup>, Fabrizio D'Amico<sup>1,2</sup> and Leonardo Palombi<sup>2,3</sup>, Carlo Bellecci<sup>1,2</sup>, Pasqualino Gaudio<sup>1,2</sup>

1. ASSOCIAZIONE ENEA-EURATOM per la FUSIONE, Department of Industrial Engineering, University of Rome "Tor Vergata", Via del Politecnico 1, 00133 Rome, (Italy)
2. International Master Courses in Protection Against CBRNe events, Department of Industrial Engineering and School of Medicine and Surgery, University of Rome Tor Vergata ([www.mastercbrn.com](http://www.mastercbrn.com))
3. Department of Biomedicine and Prevention, School of Medicine and Surgery, University of Rome Tor Vergata, Via di MontPellier 1, 00133 Rome, (Italy)

Corresponding author: Andrea Malizia, PhD – [malizia@ing.uniroma2.it](mailto:malizia@ing.uniroma2.it)

*Abstract:* - The radiological risk is related to a wide range of activities, beginning with the medical and military ones and including those connected to the industrial and research activities such as nuclear fusion. A valid tool to predict the consequences of the accidents and reduce the risk is represented by computing systems that allow modeling the evolution of a possible release of radioactive materials over time and space. In addition to proprietary codes there are free license codes, like Hot-Spot, that allow providing a set of tools to simulate diffusion in case of accidents involving radioactive materials and analyze the safety and security of the facilities in which the radioactive material is manipulated. The case studies scenario's consists in two simulations accidents scenario the first to biomass plant and the second at nuclear fission plant.

The simulation of the radioactive contamination have been conducted with the code HOT SPOT, a free license code. The results of the simulation and data discussion will be presented in this work by the authors.

*Key-Words:* - Biomass, Nuclear Fission, Accident, Radioactive, Contamination, Cesium, Energy, Safety, Security, DSS

## 1 Introduction

Nowadays the Decision Support Systems (like software) to support experts during the emergency planning operations in case of an unconventional events (like a radioactive diffusion) are one of the key safety and security issue of the new millennium. The accidents, (either intentional or natural) that cause a negative impact on environment and human health, are increasing proportionally to the needs of energy of human society. Chernobyl and Fukushima are just two examples of contaminations that have provoked short term and long term negative consequences. The DSS are necessary not only to guarantee the correct chose of safety way out that increase the safety of operators and population in case of accident but also to improve the prevention phase that is essential in an emergency planning system. The work has been developed in the context

of the activities of the International Master Courses in Protection Against CBRNe events and realized by experts (the students of the Master) coming from Academic Entities and also from Minister of Interior and Ministry of Defence. According to the high cost of the DSS officially used by these Ministers, the authors decide to test free license tools to demonstrate their functionality in case of emergency. The free license code used in this work is HOT SPOT code, it was used to simulate different type of radioactive accident scenarios and the diffusion of contamination in open field. The authors decide to simulate two different types of accidental events: 1) a biomass plant from energy production that use combustible taken in the neighborhood of Chernobyl and contaminated with <sup>137</sup>Cs due to the radioactive fallout [1-3].The geographical area considered to simulate this scenario has been an industrial area of Piemonte (Italy region) full of biomass plants. 2) The

radiological accident in the reprocessing plant at Tomsk, which occurred on 6th April 1993 during the reprocessing of irradiated reactor fuel at the Siberian Chemical Enterprise (SCE) in the Radio Chemicals Work (RCW) facility at Tomsk-7 that is has been widely described in the International Atomic Energy Agency publication "Radiological accident in the reprocessing plant at Tomsk in 1993. The HOT SPOT code has been used in the present paper to simulate the radioactive diffusion due to at two case studies accident. In this paper, the scenario together with the main results of the simulations will be presented, analyzed and discussed to understand the real possibility to use HOT SPOT as DSS during the prevention and/or intervention emergency phases.

## 2 Problem Formulation

### 2.1 Case study 1

Large parts of north-eastern Europe have been subject to fallout of radioactive nuclides "fallout" after the Chernobyl accident. These radioactive nuclides have been deposited on the ground at concentrations highly variable from area to area depending on the weather conditions and orography [1-3].

Many years after the event, the Cs-137 remains the dominant radionuclide contamination, since it has a medium half-life (30 years) and it is characterized by a high mobility in the environment.

The cesium is "moving" in ecosystems contaminated by passing from an array to another: from the atmosphere to the water and from the water back to the plants, soils, animals, humans and so on. If the radionuclides deposited on the ground, as a consequences of rain events, pass from the surface layers to the deeper ones becomes chemically available for roots uptake by trees. It happened after the nuclear disaster at Chernobyl, cesium has reached the deeper layers of the ground and has been "uptake" from the roots of forest trees thanks to competition mechanisms with the potassium ion, and the roots metabolize it [4].

The degree of contamination is different depending on whether and if the lands are cultivated or not. In farmlands, the continuous mixing causes the cesium homogenous distribution in various ground layers; if the land is not cultivated, the cesium has time to sink from the surface layers to the deep ones. The factors that make the ground a potential source of release are manifold: the composition of the soil in the percentage of clay and organic components, the pH, etc. .

Between the ground and the roots is established a balance of trade, maintained by the so-called "ionic labile pool" of ground which serves to provide bio-available elements for the roots.

For those that are its chemical characteristics, the cesium in the ground is available only in a soluble form. It is absorbed by the roots of the plants that, with a delay of a few years, achieve a certain amount of cesium in the wood of trees grown on the contaminated ground.

Since of the half-life of cesium-137 about 30 years, it is still possible to detect the presence of radioactive material in the timber from areas affected by the Chernobyl disaster.

It has been decided to simulate the consequences of an accident in a biomass plant for energy production using combustible coming from areas situated in the neighborhood of Chernobyl. It has been choose the Piemonte a region north Italy of because of its high density of biomass plants (see Figure 1).

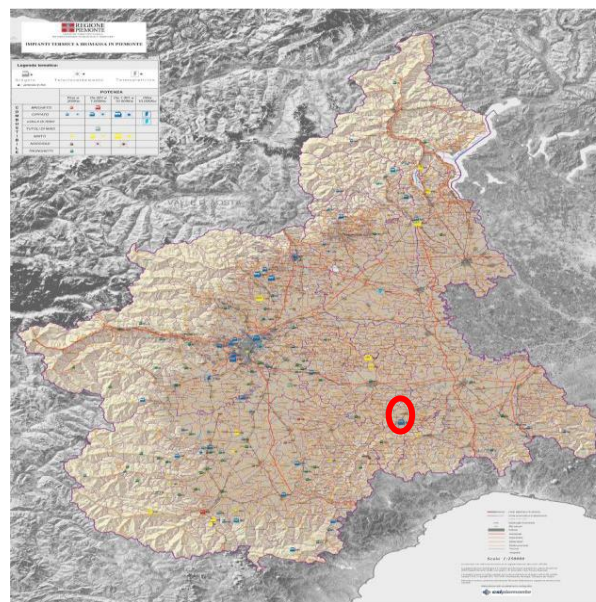


Fig.1. Map of thermic plants in Piemonte. The red box represent the selected point in which the accidents has been simulated

The biomass plant selected for the simulation has an estimated medium annual consume of 3680 m<sup>3</sup> of wood combustible ("cippato"). The plant is active 130 days per year and the estimated daily medium consume of wood combustible is 28 m<sup>3</sup> (almost 8400 Kg considering that a combustible with a medium weight of 300 Kg/m<sup>3</sup> and a humidity of 40%).

The height of emission point of the plant has been estimated at 15m with a diameter of 60cm in agreements with the real data of the plants.

The accident scenarios simulated are dispersion of <sup>137</sup>CS from chimney in different conditions

## 2.2 Case study 2

The reprocessing procedure for spent nuclear fuel in the RCW (Recirculated Cooling Water) facility requires subsequent steps in which irradiated standard uranium blocks were loaded into vessels and dissolved in concentrated nitric acid [28]. The resulting solution transferred to other vessels where it was prepared for extraction by adjusting the acidity and temperature. The stainless steel vessels, which had a volume of 34 m<sup>3</sup> and incorporate a steam heating and cooling sleeve, were located in a series of cells below the ground level, with 2m thick concrete walls and a concrete roof. During this process, an essential step represented by the insufflation of compressed air in the vessel, which is necessary to ensure the mixing of the different solutions in order to avoid:

- The separation of the solutions;
- The exergonic reaction between the nitric acid solution and the organic solvent, mainly TBP (tributylphosphate).

This is a very critical step because a lack of compressed air is one of the main causes of the accident and it is not possible to determine if it due to a human error or a plant failure. This phenomenon was the cause at Toms-7 of the energetic reaction between nitric acid and the organic substances that provoked an increase of temperature and increase of gas production. The operators endeavors to depressurize the vessel through adjacent installations were unsuccessful because the amount of gas was higher than the one that could be vented through the stack so under these conditions the pressure rose up to 18 atm leading to the rupture of the vessel. The resulting shock wave was sufficiently intense to raise and displace the concrete slabs forming the roof of the cell causing a structural damage to the equipment room above. A schematic representation of the installation involved in the accident is showed in Figure 2. [28]

According to the technical documentation, during the accident the solutions in the vessel involved in the explosion was supposed to contain a total of:

- 449 ± 120 g of Plutonium (specific activity of 2,3 TBq/kg) ;
- 8757 ± 286 kg of Uranium (specific activity of 12.4 MBq)

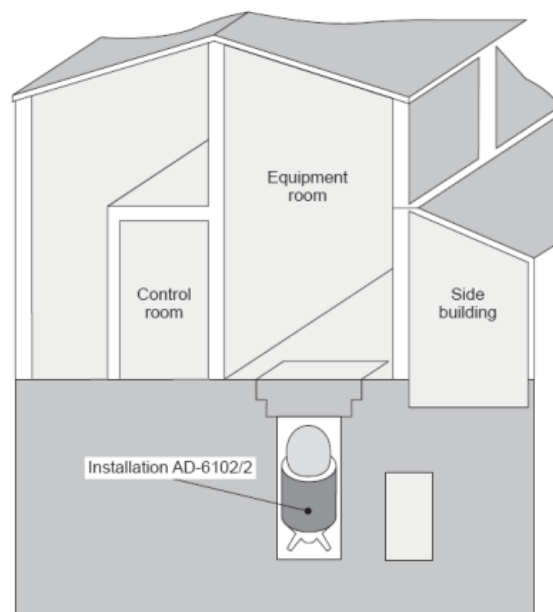


Fig. 2 : Schematic diagram of the installation which shows the location of the vessel and the rooms above involved in the accident[28]

Corresponding to total activities of 1.0 TBq and 0.11TBq respectively [29].

These data are in contrast with those obtained from the cleanup operations conducted after the accident where:

- 577± 117 g of Plutonium
- 8707 ± 350 kg of Uranium

and were collected from the installation and the cell in which they were located. The authors of the IAEA report [28] state that this discrepancy may be due to the fact that part of the material recovered after the accident originated by previous extraction cycles.

A month after the accident, soil samples were collected for the assessment of the ground contamination on the SCE site and its proximity. The total beta and gamma activity detected was 4.3 TBq whose main contribution was due to the following radionuclides: 0.04TBq of <sup>103</sup>Ru, 0.92 TBq of <sup>106</sup>Ru, 0.80 TBq of <sup>95</sup>Zr and 2.54 TBq of <sup>95</sup>Nb

In order to estimate the total activity released during the accident two models, based on the extrapolations derived from the levels of contamination, have been used. Both these models based on the Risø PUFF diffusion model, a three-dimensional model which simulates the release of Gaussian pollutant puffs predicting their concentration as they diffused and affected downwind by a horizontally homogeneous time-dependent wind, taking into account atmospheric characteristics such as turbulence intensity, potential temperature gradient, buoyant

heat flux and maximum mixing depth [30]. The first model (Model 1) makes the assumption of a release time of 15min and incorporated measurements of the radionuclide content taken from 11 snow samples

[31], while the second (Model 2) makes the assumption of an instant time release and incorporated measurement from 120 samples of snow and soil taken from 16 profiles across the area [32]. Estimates of the amount of different radionuclides evaluated from these two models are shown in table 1.

Radionuclide	Model 1	Model 2
	activity (Tbq)	activity (Tbq)
<sup>106</sup> Ru	11.1	7.9
<sup>103</sup> Ru	0.37	0.34
<sup>95</sup> Nb	17.4	11.2
<sup>95</sup> Zr	7.8	5.1
<sup>14</sup> Ce	-	0.37
<sup>144</sup> Ce	-	0.24
<sup>125</sup> Sb	-	0.10
<sup>239</sup> Pu	$7.4 \cdot 10^{-3}$	$5.2 \cdot 10^{-3}$
<b>Total</b>	<b>36.7</b>	<b>25.3</b>

Tab. 1 : Estimated activity (Tbq) released during the accident [28].

The releases due to the accident started in two different places:

1. through breaches in the walls at a height of 15-30 m which accounted for 50-60% of the activity released,
2. the roof at a height of 100-150 m.

Furthermore, the measurement of the ground contamination showed a singularity consisting in the presence of two maxima in the deposited activity across the contaminated area at right angles to the direction of the release at distances up to 12km from the Radio Chemical Works (RCW).

The authors of the report state that this pattern could be explained assuming that the release originating from the roof and the walls of the RCW are combined together with the wind directions which, for the different heights are considered different (190 degrees at ground level and 210 degrees at 100-200m height) [28].

## 3 Materials and methods

### 3.1 HOTSPOT code

The HotSpot Health Physics code and HotSpot codes are aimed at providing emergency response personnel and emergency planners with a fast, field-portable set of software tools for evaluating incidents involving radioactive materials [5]. The software is also used for safety analysis of facilities handling radioactive materials.. It is designed for near-surface releases, short-range (less than 10 km) dispersion, and short-term (less than 24 hours) release duration. The HotSpot codes are continuously updated to incorporate the most current and approved radiological dose conversion data and methodologies. These codes are based on the well-established Gaussian Plume Model (GPM). Main advantages of the Gaussian plume models are: 1) short computation time, 2)extensive validation and broad acceptance worldwide. For the evaluation of radiological scenarios, HotSpot uses the methods of radiation dosimetry recommended by the International Commission on Radiological Protection (ICRP) [6] and the US Environmental Protection Agency's (EPA) Federal Guidance Reports No. 11, 12 and 13 [7-9]. In order to simulate different meteorological conditions HOT SPOT allows the selection of the Pasquill classes.

#### 3.1.1 Pasquill Classes used in HOT SPOT

Meteorologists distinguish several states of the local atmosphere: A, B, C, D, E, F. These states can be tabulated as a function of weather conditions, wind speed and time of day. According to the stability class, the attack can result in a wide spectrum of lethal effects. Therefore, the potential terrorist will certainly consider those, just as it happens by war-planners, so that the lethal effects are maximized. The stability of the atmosphere depends on the temperature difference between an air parcel and the air surrounding it. Therefore, different levels of stability may depend on the temperature difference between the air Parcel and the surrounding air. [10-11].

The stability classes used for this work are referred to Pasquill – Gifford stability [10]. Stability classes A, B, and C refer to daytime hours with unstable conditions. Stability D is representative of overcast days or nights with neutral conditions. Stabilities E and F refer to night time, stable conditions and are based on the amount of cloud cover. Thus, classification A represents conditions of the greatest instability, and classification F reflects conditions of the greatest stability.



### 3.2 SELECTION OF BOUNDARY CONDITIONS

#### 3.2.1 Case study 1

The authors, expert in simulation of unconventional events [12-19, 24-27], choose the model “General Plume” to simulate the accident that is ideal for the radioactive release from a chimney [17,19,23]. After that the principal boundary conditions has been uploaded in the GUI (Graphical User Interface) of the software (see Figure 3).

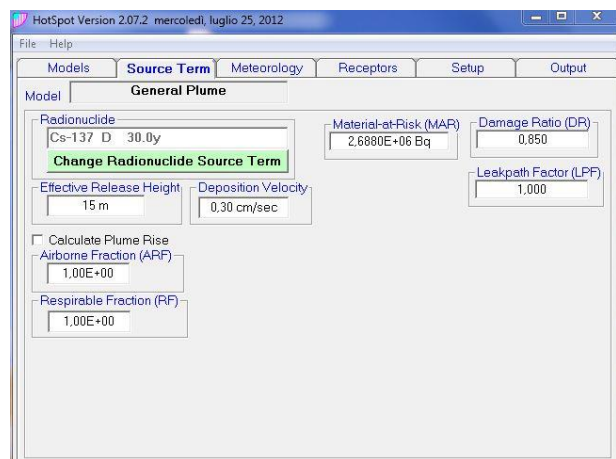


Fig.3. Source term condition uploaded in HOT SPOT GUI

In order to estimate the contamination values of <sup>137</sup>Cs in the wood has been considered the data from a technical report by University of Pavia [20]. The maximum level of contamination detected have been 320 Bq/Kg for combustible wood (“cippato”) and 40000 Bq/Kg for ashes. The combustion of wood generates 85% of volatile substances, the 14% of carbon and the 1% of ashes so in the simulation the authors consider only the activity of combustible wood as value of contamination. The reality, as reported in [21], the use of ashes is considered the worst for human health, but it is not considered in this work.

The accident scenarios simulated have been two. In table 2 are reported the two different meteorological conditions:

Scenario	Wind speed (at 15 m)	Stability Class	Wind Direction
1	3 m/s	C	225 (from SW)
2	0,5 m/s	D	225 (from SW)

Tab. 2. Meteorological conditions

For both the scenarios, the height of the emission point is 15 meters and the sampling times has been fixed at 30 minutes. The DFC library used is the

FGR 11 that allows to include the phenomena of reflection on ground and resuspension of particulate [23]. The value of the mean respiratory flux has been fixed at  $3,33 \times 10^{-4} \text{ m}^3/\text{s}$  (as described for a population with a medium intensity activity). The values of TEDE (Total Effective Dose Equivalent) as sum of equivalent dose for each organ in the body (both for external and internal deposition) have been added together with the values of radioactivity on the ground (see Figure 4).

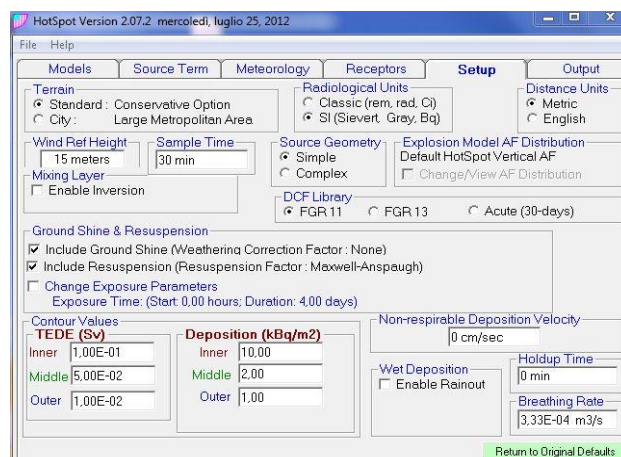


Fig.4. Setup condition uploaded in HOT SPOT GUI

The boundary conditions foresee also three different bands: internal, medium and external, that are graphically represented as three different zones of the plume in the contaminated zone. The TEDE and the ground deposition represent the values of highest interest for an analysis on radioactive particulate contamination. The last boundary condition selected has been the modality “compass” on data output that allows a representation of all the area potentially involved during the contamination in accordance with wind variation [18,19].

#### 3.2.1 Case study 2

During the release took place the wind was blowing at a speed of 8-13 m/s, from a southwesterly direction and due to the snow that was falling [28] the sky must have been highly overcast; these two variables affect the spread of the contamination due to an atmospheric release. A parameter which takes into consideration these meteorological aspects to define the turbulence status of the system under investigation is the Pasquill’s stability class which is also a parameter used in the HotSpot code. In this particular case, the meteorological conditions during the accident are coherent with the Pasquill’s stability class “D” which means the absence of turbulence. The falling snow also increased the dry

deposition velocity of the particles released of a factor of ten taking into account also the dry deposition velocity estimated to be  $1,0 \times 10^{-3} \text{ ms}^{-1}$ , in fact the estimated deposition velocity for all the gamma and beta emitters varied between 0.15 and  $0.20 \text{ ms}^{-1}$ . The HotSpot model chosen for the benchmark was “General Explosion”. This model allows the user to specify the quantity of high explosive (TNT equivalent) which caused the explosion; the default value of the code is 1 lb (a conservative estimate of the TNT equivalent of an exploding vehicle gas tank [33] which resulted appropriate also for simulating the rupture of the vessel due to the high pressure). The IAEA report did not provide sufficient data regarding the initial content of  $^{106}\text{Ru}$ . It did provide the estimated activity released during the accident according to two different dispersion models which ranged between 7.9 and 11.1 TBq. Starting from this experimental evidence, the authors selected the mean value of 9.5 TBq supposed to be an appropriate value for the “Source Term”. Furthermore, since this was an estimate of the  $^{106}\text{Ru}$  already deposited on the ground, the default value of 1.0 for the Damage Ratio (the fraction of the MAR actually impacted in the release scenario) has been chosen, meaning that all the MAR was released. Since the explosion created a breach in the roof and side walls of the installation, no filtration mechanism could have mitigated the release of the MAR. The software evaluates this feature in terms of “Leakpath Factor” ( i.e. the fraction of the MAR that passes through some confinement or filtration mechanism: a value of 1.0, chosen for the benchmark, is representative of the absence of such mechanisms). The Deposition Velocity estimated for the deposition of the beta-gamma emitters was of about  $0.20 \text{ ms}^{-1}$  [34] and this was the value chosen for the benchmark. As mentioned above, the simulations were divided in two distinct groups of scenario named “Simulations 190°” and “Simulations 210°” with regard to the different wind directions assuming the release of the 65% of the total  $^{106}\text{Ru}$  activity and the release of 35% of the total  $^{106}\text{Ru}$  activity (6,175 TBq and 3,325 TBq respectively). The “General Explosion” one does not allow the user to set the release height. The only parameters introduced to “simulate” different meteorological conditions at different height were the wind speed ( $5 \text{ ms}^{-1}$  and  $10 \text{ ms}^{-1}$ ) and the stability Pasquill classes D and C, which are the first and second more probable stability classes for the height of 20 and 125 m [35] (used in the simulations as mean value for the release height). Furthermore, for each scenario, different sample times have been

considered. Finally, since the duration of the release could not be assessed during the accident, two different sample times have been chosen for each simulation in order to evaluate both: an instantaneous (1min sample time) and time protracted release (10min sample time). Options and values for the simulations are shown in Table 3 and Table 4.

Simulations 190°								
Model General Explosion								
Source Term								
Radionuclide	Ru-106 W 368.2 d							
Material-at-Risk	6,175 TBq							
Deposition Velocity	20 $\text{cms}^{-1}$							
Meteorology	Simulation 190° D				Simulation 190° C			
	190° D WS 5 $\text{ms}^{-1}$		190° D WS 10 $\text{ms}^{-1}$		190° C WS 5 $\text{ms}^{-1}$		190° C WS 10 $\text{ms}^{-1}$	
10-meter-wind-speed	5 $\text{ms}^{-1}$		10 $\text{ms}^{-1}$		5 $\text{ms}^{-1}$		10 $\text{ms}^{-1}$	
Wind Direction	190°		190°		190°		190°	
Stability Class	D		D		C		C	
Setup	ST 10 min	ST 1 min	ST 10 min	ST 1 min	ST 10 min	ST 1 min	ST 10 min	ST 1 min
Sample time	10 min	1 min	10 min	1 min	10 min	1 min	10 min	1 min
Non-respirable Deposition Velocity	20 $\text{cms}^{-1}$	20 $\text{cms}^{-1}$	20 $\text{cms}^{-1}$	20 $\text{cms}^{-1}$	20 $\text{cms}^{-1}$	20 $\text{cms}^{-1}$	20 $\text{cms}^{-1}$	20 $\text{cms}^{-1}$

Tab. 3: Options and values for: a) Simulations 190°(unmodified HotSpot default values are not shown).

Simulations 210°								
Model General Explosion								
Source Term								
Radionuclide	Ru-106 W 368.2 d							
Material-at-Risk	3,325 TBq							
Deposition Velocity	20 $\text{cms}^{-1}$							
Meteorology	Simulation 210° D				Simulation 210° C			
	210° D WS 5 $\text{ms}^{-1}$		210° D WS 10 $\text{ms}^{-1}$		210° C WS 5 $\text{ms}^{-1}$		210° C WS 10 $\text{ms}^{-1}$	
10-meter-wind-speed	5 $\text{ms}^{-1}$		10 $\text{ms}^{-1}$		5 $\text{ms}^{-1}$		10 $\text{ms}^{-1}$	
Wind Direction	210°		210°		210°		210°	
Stability Class	D		D		C		C	
Setup	ST 10 min	ST 1 min	ST 10 min	ST 1 min	ST 10 min	ST 1 min	ST 10 min	ST 1 min
Sample time	10 min	1 min	10 min	1 min	10 min	1 min	10 min	1 min
Non-respirable Deposition Velocity	20 $\text{cms}^{-1}$	20 $\text{cms}^{-1}$	20 $\text{cms}^{-1}$	20 $\text{cms}^{-1}$	20 $\text{cms}^{-1}$	20 $\text{cms}^{-1}$	20 $\text{cms}^{-1}$	20 $\text{cms}^{-1}$

Tab. 4: Options and values for: a) Simulations 210°(unmodified HotSpot default values are not shown).

The ground contamination data available for  $^{106}\text{Ru}$  have been detected at the distance of 4.5km, 7.0km and 12.0km in a northwesterly direction from the point of the release. For this reason, the default values for the “Receptors” were modified in order to obtain the x and y coordinates which corresponded to those downwind distances for both wind directions ( $190^\circ$  and  $210^\circ$ ): their values are shown in Table 1. The z coordinate, which identifies the receptor’s height from the ground has a default value of 1.5m, this value has not been modified since it is irrelevant when analyzing the ground deposition. Values of x and y coordinates for downwind distances of 4.5km, 7.0km and 12.0km for the two wind directions  $190^\circ$  and  $210^\circ$  are shown in Table 5.

Downwind distance	Simulations $190^\circ$		Simulations $210^\circ$	
	x (km)	y (km)	x (km)	y (km)
Km				
4.5	0,718	4,432	2,250	3,897
7.0	1,216	6,894	3,500	6,062
12.0	2,084	11,818	6,000	10,392

Table 4 : Spatial coordinates for downwind distance of 4.5 km, 7.0 km and 12.0 km.

## 4 Problem Solution

### 4.1 Case study 1

#### 4.1.1 Results of Accident Scenario 1

The first result analyzed (figure 5) is the general plume graph (represented in a polar coordinate system the release point located at axes origin). It is a picture of the plume at the end of the observation period (30 minutes).

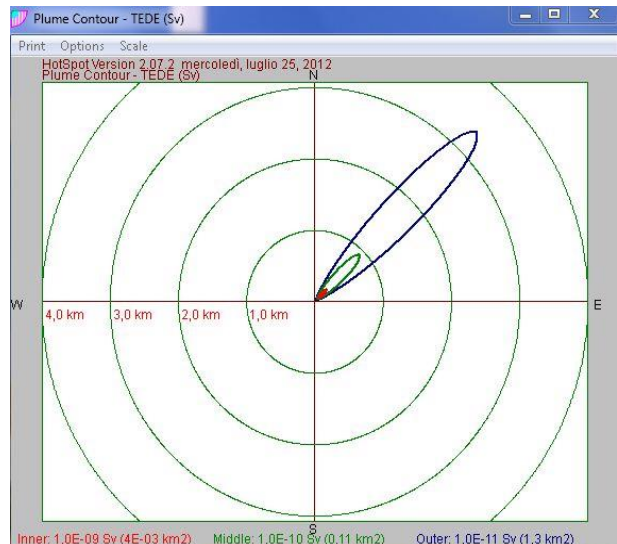


Fig.5. Plume at 30 minutes (Scenario 1)

In the figure 6 it is represented the variation of equivalent dose (in Sievert) with the distance from the release point. The “receptor height” has been fixed at 1,5 meter (the breathable zone of a medium height zone) and so it is evident that the maximum of dose value is calculated at 100 meters from the release point.

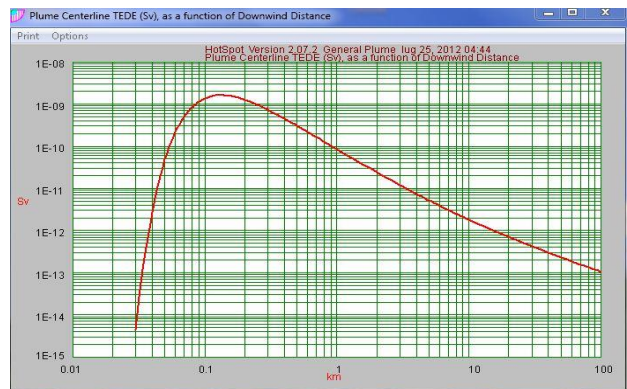


Fig.6. (Scenario 1) TEDE (in Sv) variation from the release point (height of 1,5 meters)

In the figure 7 the variation with the distance of the ground deposition values is showed.

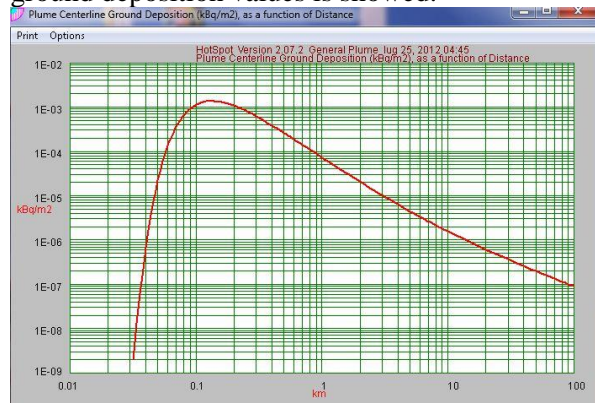


Fig.7. (Scenario 1) TEDE (in Sv) variation from the release point (ground level)



The table 5 shows all the output values from HOT SPOT.

DISTANCE km	T E D E (Sv)	RESPIRABLE TIME-INTEGRATED AIR CONCENTRATION (Bq-sec)/m3	GROUND SURFACE DEPOSITION (kBq/m2)	GROUND SHINE DOSE RATE (Sv/hr)	ARRIVAL TIME (hour:min)
0,010	0,0E+00	0,0E+00	0,0E+00	0,0E+00	<00:01
0,030	4,4E-15	1,5E-03	2,2E-10	0,0E+00	<00:01
0,070	5,0E-10	1,5E+02	3,6E-04	7,2E-13	<00:01
0,100	1,4E-09	3,9E+02	1,1E-03	2,2E-12	<00:01
0,200	1,3E-09	3,6E+02	1,1E-03	2,2E-12	00:01
0,300	7,3E-10	2,1E+02	6,2E-04	1,2E-12	00:01
0,400	4,5E-10	1,3E+02	3,9E-04	7,7E-13	00:02
0,500	3,0E-10	8,7E+01	2,6E-04	5,2E-13	00:02
0,600	2,2E-10	6,3E+01	1,9E-04	3,7E-13	00:03
0,700	1,7E-10	4,7E+01	1,4E-04	2,8E-13	00:03
0,800	1,3E-10	3,7E+01	1,1E-04	2,2E-13	00:04
0,900	1,0E-10	3,0E+01	8,9E-05	1,8E-13	00:05
1,000	8,6E-11	2,4E+01	7,3E-05	1,5E-13	00:05
3,000	1,2E-11	3,4E+00	1,0E-05	2,1E-14	00:16
5,000	1,2E-12	1,5E+00	4,4E-06	8,8E-15	00:27
10,000	1,8E-12	5,2E-01	1,5E-06	3,1E-15	00:55
20,000	7,0E-13	2,0E-01	6,0E-07	1,2E-15	01:51
40,000	3,0E-13	8,5E-02	2,6E-07	5,1E-16	03:42
60,000	1,9E-13	5,3E-02	1,6E-07	3,2E-16	05:33
80,000	1,3E-13	3,8E-02	1,2E-07	2,3E-16	07:24

Tab.5. (Scenario 1) Output value from HOT SPOT

### 4.1.2 Results of Accident Scenario 2

The Accident Scenario 2 presents a variation in meteorological conditions (the stability class D has been uploaded in this case). It has been selected to analyze variation between 2 stability classes different in terms of wind speed [10]. In the figure 8 the general plume is showed.

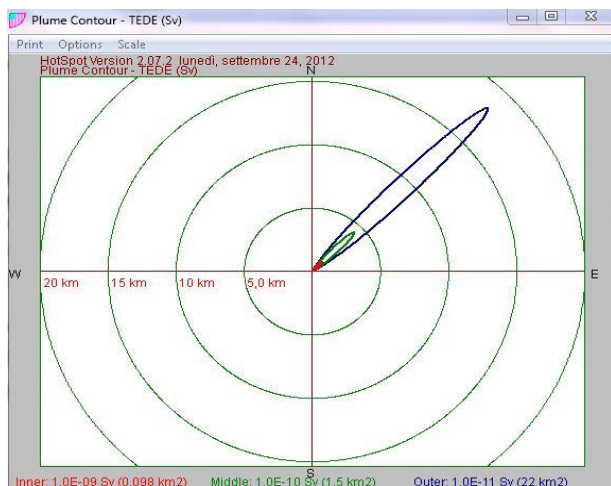


Fig.8. Plume at 30 minutes (Scenario 2)

Moreover, the figure 9 and 10 show, respectively, the ground deposition with a receptor height of 1,5 meters (breathable area) and at ground level.

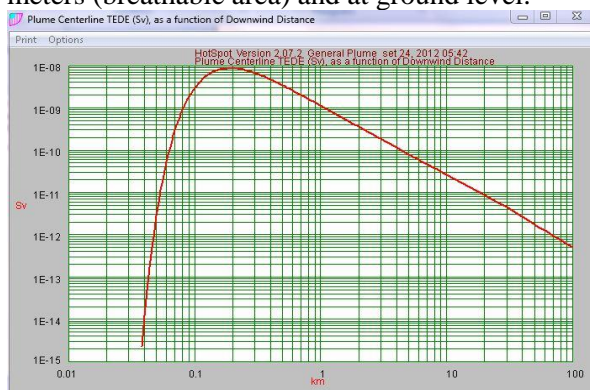


Fig.9. (Scenario 2) TEDE (in Sv) variation from the release point (height of 1,5 meters)

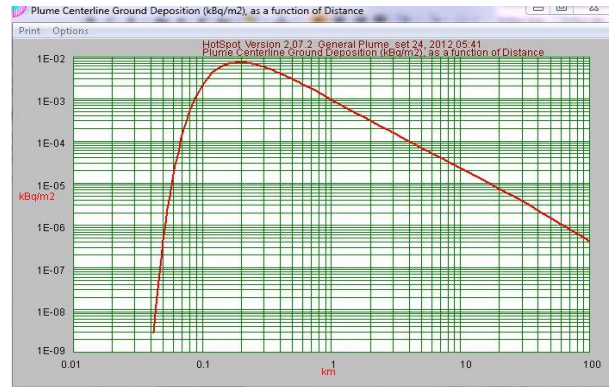


Fig.10. (Scenario 2) TEDE (in Sv) variation from the release point (ground level)

### 4.3 Results and Analysis

The comparison between the two different scenarios shows that the plume area of Scenario 2 are wider than the one in Scenario 1 and the plume is extended in a larger surface but the contamination values are negligible for this second scenario.

The results of the case study 1 simulations show that the maximum value of contamination is detected at a distance of 130 meters from the release point (and is  $9,61 \times 10^{-6}$  mSv). The maximum value of ground contamination is lower than  $1 \text{ Bq/m}^2$  (Scenario 1) and  $10 \text{ Bq/m}^2$  (Scenario 2).

The figure 11 shows a projection of the possible fallout in case of accident (in the worst scenario in absence of wind). Taking into account the prevalent wind in the considered area, the fallout zone can be delimited by two red lines (see figure 10).

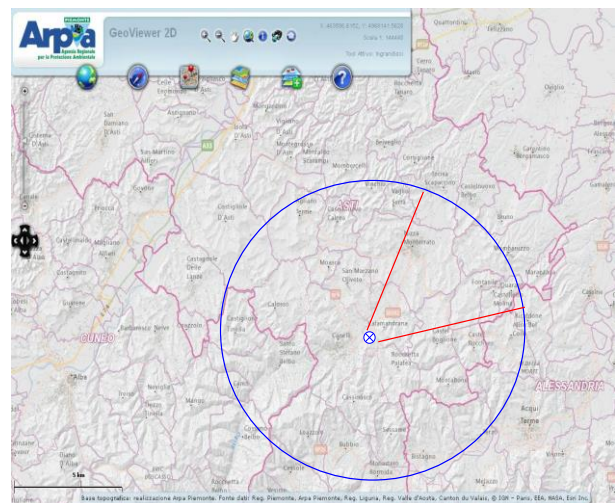


Fig.11. Delimitation of the possible fallout zone

The cumulative dose obtained is  $6 \times 10^{-2}$  Sv/year, that is a value lowest than the one imposed by Italian Law [22,23].



### 4.1 Case study 2

The outputs generated by HotSpot with the sixteen combinations of values and options (Table 6) have been analyzed in order to find which combination was the more appropriate to describe the pattern and the amount of ground contamination with <sup>106</sup>Ru. As shown in Table 6 a wind speed of 5 ms<sup>-1</sup> associated to the Pasquill stability class “D” and a sample time of 1 min give a good match with the experimental data (Figure 12). Figure 12 showed the values of activity (kBq·m<sup>-2</sup>) for ground deposition of <sup>106</sup>Ru at distance of : 4.5 km; 7.0 km; 12.0 km, computed by the HotSpot code with the options and values for the 5ms<sup>-1</sup> wind speed (left) showed the best match with the experimental data for the ground contamination with <sup>106</sup>Ru across the path of the fallout at different distances from the RCW (right)

Benchmark for ground contamination with <sup>106</sup> Ru							
Wind speed 5 m·s <sup>-1</sup>			Wind speed 10 m·s <sup>-1</sup>				
Model	General Explosion		General Explosion				
Source Term							
Radionuclide	Ru-106 W 368.2		Ru-106 W 368.2				
Meteorology							
10-meter-wind-speed	5 m·s <sup>-1</sup>		10 m·s <sup>-1</sup>				
Stability Class	D		D				
Setup							
Sample time	1 min		1 min				
Downwind distance							
	190°			190°			
Km	x (km)	y (km)	kBq·m <sup>-2</sup>	x (km)	y (km)	kBq·m <sup>-2</sup>	
4.5	0,718	4,432	<b>690</b>	0,718	4,432	<b>700</b>	
7.0	1,216	6,894	<b>240</b>	1,216	6,894	<b>310</b>	
12.0	2,084	11,818	<b>55</b>	2,084	11,818	<b>110</b>	
	210°			210°			
Km	x (km)	y (km)	kBq·m <sup>-2</sup>	x (km)	y (km)	kBq·m <sup>-2</sup>	
4.5	2,250	3,897	<b>380</b>	2,250	3,897	<b>380</b>	
7.0	3,500	6,062	<b>130</b>	3,500	6,062	<b>150</b>	
12.0	6,000	10,392	<b>30</b>	6,000	10,392	<b>57</b>	

Tab. 6: Option and values of the benchmark showing the best correlation with the experimental values for the ground contamination with <sup>106</sup>Ru.

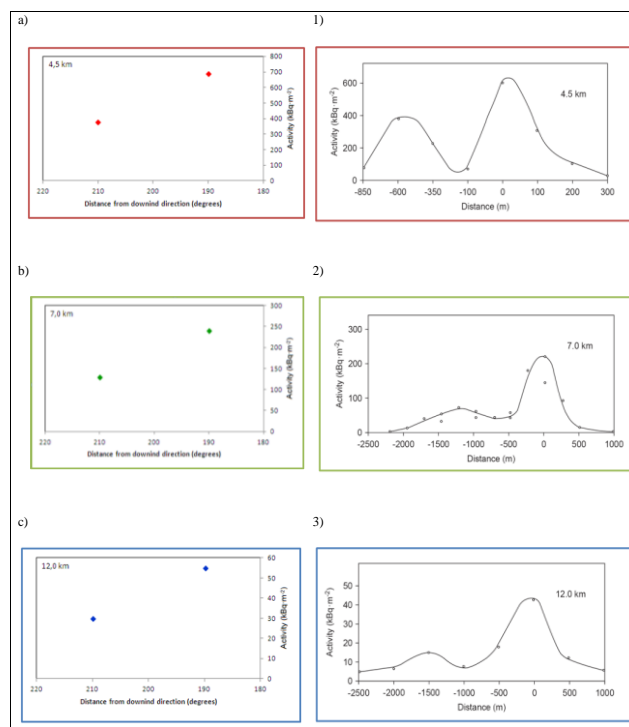


Figure 12 Values of activity (kBq·m<sup>-2</sup>) for ground deposition of <sup>106</sup>Ru at distance of 4.5 km, 7.0 km and 12.0 km.

The HotSpot software also allows the user to visualize both the TEDE contour plots and Ground Deposition Contour Plots which show the downwind and crosswind contours for dose levels and for the extent of the deposition respectively, and the TEDE Graph and Ground Deposition graph which display the relative values as a function of plume centerline downwind distance. The Ground Deposition contour plots for the two scenarios described in table 6 are shown in figure 13.

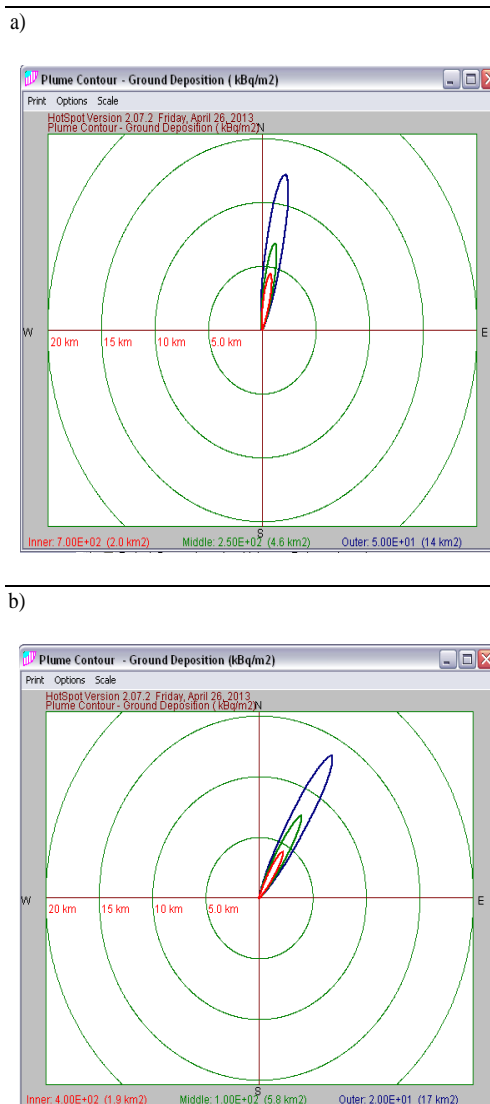


Fig. 13: Ground Deposition contour Plot for the two scenarios described in table 5 for wind direction  $190^\circ$  (a) and  $210^\circ$  (b). The contour values for the plume are  $7.0E+02$  (inner),  $2.5E+02$  (middle) and  $5E+01$  (outer) for direction  $190^\circ$  and  $4.0E+2$  (inner)  $1.0E+02$  (middle) and  $2.0E+01$  (outer) for direction  $210^\circ$

## 5 Conclusion

The simulation of the events and the evolution of the plume were realized through the hotspot software. This software takes into account the weather conditions, the wind direction, the stack height, respiration, but does not take into account the topography of the area, the presence of buildings and / or obstacles to the advancement of the plume and the presence any updrafts.

In the case studies that we have examined the area is flat and free of large buildings. Furthermore, the area is near the sea and it is not characterized by abnormal turbulences. According to that, the simulations improved should be closer to the reality. It should be said that the simulations performed with

the software do not always consider all the parameters and variables that could affect the evolution of the plume. This code needs very little time for calculations (less than 1 minute) and very conservative estimations can be obtaining starting from very few initial information. The authors can affirm that the software can be used as a useful DSS to assist the decision maker, but cannot fully replace it. In case of an accident, however, the real measurements should be carried out to verify the goodness of the simulated data.

Considering an event as the accident described, since the dose values calculated are very low (around an order of magnitude lower than the LAW limit), the approximations and the margin of error due to the simulation should not significantly alter the final results. At the conclusion of this study, we can say, with a good degree of reliability, that scenarios as the one proposed would constitute events without any radiological significance for the population and for the workers.

The Hot Spot code could certainly be used also in the processes of:

- Prevention;
- Risk planning;
- Support the decision-making process during the accidental events.

## References:

- [1] United Nations Scientific Committee on the Effect of Atomic Radiation (UNSCEAR). *Report sources and effects of ionizing radiation*. UNSCEAR Report to the General Assembly Volume II, Annex J, 2000.
- [2] International Atomic Energy Agency (IAEA). *Summary Report on the Post-Accident Review Meeting on the Chernobyl Accident*. Safety Series 75, Vienna, 1986.
- [3] International Atomic Energy Agency (IAEA). *Generic Models for use in assessing the impact of discharges of radioactive substances to the environment*. Safety Reports Series 19, Vienna, 2001.
- [4] Voigt, G. and Fesenko, S. *Radioactivity in the environment. Remediation of contaminated environments*. Elsevier editor, 2009.
- [5] Homann S.G. and Aluzzi F. *HotSpot Health Physics Codes Version 3.0 User's Guide*. National Atmospheric Release Advisory Center Lawrence Livermore. National Laboratory Livermore, CA 94550, 2013.
- [6] International Commission on Radiological

- Protection (ICRP). *Basis for Dosimetric Quantities Used in Radiological Protection*. ICRP, Ottawa, Canada, 2005.
- [7] Environmental Protection Agency (EPA). *Limiting Values Radionuclide Intake and Air Concentration, and Dose Conversion Factors for Inhalation, Submersion, and Ingestion*. EPA, Federal Guidance Report 11, Washington DC, 1988.
- [8] Environmental Protection Agency (EPA). *External Exposure to Radionuclides in Air, Water, and Soil*. EPA, Federal Guidance Report 12, Washington DC, 1993.
- [9] Environmental Protection Agency (EPA). *Cancer Risk Coefficients for Environmental Exposure to Radionuclides*. EPA, Federal Guidance Report 13, Washington DC, 1999.
- [10] Rentai, Y. Atmospheric dispersion of radioactive material in radiological risk assessment and emergency response. *Progress in Nuclear Science and Technology*, Vol. 1, 2011, pp. 7-13.
- [11] Bellecci, C., Gaudio, P., Gelfusa, M., Malizia A., M. Richetta, C., et al. Planetary boundary layer (PBL) monitoring by means of two laser radar systems: experimental results and comparison. *In Lidar technologies, techniques, and measurements for atmospheric remote sensing VI SPIE Conference*. Vol. 7832, 2010.
- [12] Cenciarelli, O., Malizia, A., Marinelli, M., Pietropaoli, S., Gallo, R., et al. Evaluation of biohazard management of the Italian national fire brigade. *Defence S&T Technical Bulletin* Vol. 6, pp. 33-41, 2013
- [13] Gallo, R., De Angelis, P., Malizia, A., Conetta, F., Di Giovanni, D., et al. Development of a georeferencing software for radiological diffusion in order to improve the safety and security of first responders. *Defence S&T Technical Bulletin* Vol. 6, pp. 21-32, 2013.
- [14] Malizia, A., Lupelli, I., D'Amico, F., Sassolini, A., Fiduccia, A., et al. Comparison of software for rescue operation planning during an accident in a nuclear power plant. *Defence S&T Technical Bulletin* Vol. 5, pp. 36-45, 2012.
- [15] Malizia, A., Quaranta, R., Mugavero, R., Carcano, R., Franceschi, G. Proposal of the prototype RoSyD-CBRN, a robotic system for remote detection of CBRN agents. *Defence S&T Technical Bulletin* Vol. 4, pp. 64-76, 2011.
- [16-20] Malizia, A., Quaranta, R., Mugavero, R. CBRN events in the subway system of Rome: Technical-managerial solutions for risk reduction. *Defence S&T Technical Bulletin* Vol. 2, pp. 140-157, 2010.
- [17] Paziienza, M., Britti, MS., Carestia, M., Cenciarelli, O., D'Amico, F., et al. Use of Particle Counter System for the Optimization of Sampling, Identification and Decontamination Procedures for Biological Aerosols Dispersion in Confined Environment. *J Microb Biochem Technol* Vol. 6, pp. 43-48, 2013.
- [18] Cacciotti, I., Aspetti, PC., Cenciarelli, O., Carestia, M., Di Giovanni, D., et al. Simulation of Caesium-137 (<sup>137</sup>Cs) Local Diffusion as a Consequence of the Chernobyl Accident Using Hotspot. *Defence S&T Technical Bulletin* Vol. 7, pp. 18-26, 2014.
- [19] Sassolini, A., Malizia, A., D'Amico, F., Carestia, M., Di Giovanni, D., et al. Evaluation of the Effectiveness of Titanium Dioxide (TiO<sub>2</sub>) Self-Cleaning Coating for Increased Protection Against CBRN Incidents in Critical Infrastructures. *Defence S&T Technical Bulletin* Vol. 7, pp. 9-17, 2014.
- [20] Manera, S., and Milani, D. *Pellet radioattivo – indagine radiometrica e considerazioni di radioprotezione*. Università degli Studi di Pavia, 2009, <http://www-3.unipv.it/safety/radio/pellet.pdf>.
- [21] International Atomic Energy Agency (IAEA). *Assessing radiation doses to the public from radionuclides in timber and wood products*. IAEA, Vienna, Austria, 2003.
- [22] Decreto Legislativo 17 marzo 1995, n. 230. *Attuazione delle direttive 89/618/Euratom, 90/641/Euratom, 96/29/Euratom, 2006/117/Euratom in materia di radiazioni ionizzanti e 2009/71/Euratom, in materia di sicurezza nucleare degli impianti nucleari*. Gazzetta Ufficiale n.136 del 13-6-1995 - Suppl. Ordinario n. 74.
- [23] Decreto Legislativo 26 maggio 2000, n. 241. *Attuazione della direttiva 96/29/EURATOM in materia di protezione sanitaria della popolazione e dei lavoratori contro i rischi derivanti dalle radiazioni ionizzanti*. Gazzetta Ufficiale n.203 del 31-8-2000 - Suppl. Ordinario n. 140.
- [24] Malizia, A., Lupelli, I., Richetta, M., Gelfusa, M., Bellecci, C., Gaudio, P., "Safety analysis in large volume vacuum systems like tokamak: Experiments and numerical simulation to analyze vacuum ruptures consequences", *Advances in Materials Science and Engineering*, doi: 10.1155/2014/201831, 2014.
- [25] Di Giovanni, D., Luttazzi, E., Marchi, F., Latini, G., Carestia, M., Malizia, A., Gelfusa, M., Fiorito, R., D'Amico, F., Cenciarelli, O., Gucciardino, A., Bellecci, C., Gaudio, P., "Two realistic scenarios of intentional release of radionuclides (Cs-137, Sr-90) - the use of the HotSpot code to forecast contamination extent", *WSEAS Transactions on Environment and Development*, 10, 106-122, 2014.



- [26] Gaudio, P., Gelfusa, M., Malizia, A., Richetta, M., Antonucci, A., Ventura, P., Murari, A., Vega, J., "Design and development of a compact Lidar/Dial system for aerial surveillance of urban areas", Proceedings of SPIE - The International Society for Optical Engineering, 8894,, 88940D, 2013.
- [27] Gaudio, P., Malizia, A., Lupelli, I., "Experimental and numerical analysis of dust resuspension for supporting chemical and radiological risk assessment in a nuclear fusion device", International Conference on Mathematical Models for Engineering Science - Proceedings, 134-147, 2010.
- [28] "The Radiological Accident in the Reprocessing Plant at Tomsk". International Atomic Energy Agency. October 1998.
- [29] INTER-DEPARTMENT (INTER-AGENCY) COMMISSION, Inquiry of Causes and Elaboration of Measures on Mitigation of the Accident Consequences at the Radiochemical Enterprise of Siberian Chemical Enterprises (SCE), Statement of Inter-Agency Commission No. 02-07/329, 14 April 1993, Moscow and Tomsk (1993) (in Russian).
- [30] Mikkelsen, T., Larsen, S.E., Description of the Risø PUFF diffusion model, Nucl. Technol. 67 . 56-65, 1984
- [31] Andreev, G.S., Malyshkin, A.I., "Calculation of Radioactive Activity Contained in the Area outside the Industrial Zone Contaminated as a Result of Release after Destruction of the Processing Installation at the RCW on 06/04/93", Tech. Rep. SCE No. 26/1364, Tomsk-7 12 pp. (in Russian), 1993.
- [32] Savkin, M.N., Titov, A.V., "Analysis of the Radiation Situation in the Aftermath of the Accidental Release from the Radiochemical Enterprise of Siberian Chemical Enterprises, Moscow" (1995) (in Russian).
- [33] International Energy Agency, "Key World energy statistics", 2012.
- [34] Vakulovsky, S.M., Shershakov, V.M., Borodin, R.V., et al., "Analysis and prognosis of the radiation situation at the area of the accident at Siberian Chemical Enterprises", Radiation and Risk, Issue 3, Supplement 2, Moscow and Obninsk (1993) 48 pp. (in Russian).
- [35] De Marrais G. A. "Atmospheric stability class determinations on a 481-meter tower in Oklahoma". Atmospheric Environment Volume 12, Issue 10, 1978, Pages 1957-1964, 1967.